Supporting Information

Visualizing lysosomal viscosity in atherosclerosis with a long-wavelength and large Stokes shift fluorescent probe

Xue Wu, [a ‡] Junjie Kou, [a ‡] Ruixin Zhang, [a] Xiaoxuan Shi, [a] Ying Li [a*], Fanpeng Kong [a*], Chang Xu,[a*] and Bo Tang [a, b]

a College of Chemistry, Chemical Engineering and Materials Science, Key Laboratory of Molecular and Nano Probes, Ministry of Education, Shandong Normal University, Jinan 250014, People's Republic of China. b Laoshan Laboratory, Qingdao 266237, Shandong, People's Republic of China, Email: 1031208296@qq.com, kong-fanpeng@163.com, 621042@sdnu.edu.cn

Contents:

1. General Experimental Section

Materials and instruments

All of compounds used in the synthesis experiments were analytically pure, and the reagents used in the spectral tests were spectroscopically pure. ^{1}H NMR spectra were obtained at 400 MHz using Bruker NMR spectrometers, and ^{13}C NMR spectra were recorded at 100 MHz. The mass spectra were obtained using the Bruker maXis ultra-high-resolution-TOF MS system. UV-vis spectroscopy data were obtained using a UV-vis spectrophotometer (Shimadzu Corporation UV-1700, Japan). Fluorescence data were performed on a F-4600 fluorescence spectrophotometer (Hitachi, Japan) at room temperature. MTT assays was acquired with a microplate reader (RT6000, Rayto, USA). Fluorescence imaging in cells were performed with Leica TCS SP8 Confocal Laser Scanning Microscope. RAW264.7 cells were purchased from the Cell Bank of the Chinese Academy of Sciences (Shanghai, China). $ApoE^{-/-}$ mice (Male, 8 weeks old) and C57BL/6 mice (Male, 8 weeks old) was purchased from SIPEIFU (Beijing) Biotechnology. The experiment protocol was in accordance with the Principles of Laboratory Animal Care (People's Republic of China) and was approved by the Animal Care and Use Committee of Shandong Normal University (AEECSDNU2023061).

Quantum calculations

All quantum chemical calculations were performed using Gaussian 16. The ground-state geometry was optimized and confirmed as a minimum via frequency analysis at the B3LYP-D3/6-31G(d) level to describe long-range interactions accurately [1, 2]. Subsequently, the excited-state structure was optimized using Time-Dependent Density Functional Theory (TDDFT). Based on the TDDFT results, the electron-hole analysis for the target excitation was conducted using Multiwfn 3.8 to characterize the excitation nature [3]. All molecular orbitals and electron-hole distribution maps were rendered using VMD 1.9.3 for visualization [4].

Spectrophotometric Experiments

QV-S was dissolved in DMSO to prepare the stock solution with a concentration of 2

mM, storing at -4 °C and in the dark. The final concentration of **QV-S** was 10 μM. The concentration of a series of metal ions and halogen ions (Ca^{2+}, Cu^{2+}, Fe^{2+}, Fe^{3+}, K^{+}, Mg^{2+},) is 200 μM. The concentration of a series of anionic solutions (F^{-}, I^{-}, Cl^{-}, SO_3^{2-}, SO_4^{2-}, HCO_3^{-}) is 200 μM. The concentration of reducing species and amino acids (GSH, Cys, Hcy, Glu,) is 1mM. The concentration of oxidized species (H_2O_2, HClO, HS^{-},) is 200 μM unless otherwise specified.

Cell Culture

RAW264.7 cells were purchased from the Wuhan Pricella Biotechnology Co., Ltd., and cultured in Dulbecco's Modified Eagle Medium media (DMEM, Gibco) supplemented with 10% heat-inactivated fetal bovine serum (FBS, VivaCell) and 1% antibiotics (100 U/mL penicillin and 100 μg/mL streptomycin, Hyclone) at 37 °C and 5% CO_2.

Cytotoxicity Assays

The cytotoxicity of the **QV-S** to RAW264.7 cells was studied by standard microculture tetrazolium (MTT) assays. 1×10^6 cells/mL cells were seeded in 96-well plates and then incubated with various concentrations of **QV-S** (0-30 μM) for 24 h. After that, 100 μL of MTT (0.5 mg / mL) was added to each well and incubated for another 4 h. Finally, the media were discharged, and 100 μL of DMSO was added to dissolve the formazan crystals. The plate was shaken for about 10 min, and each well was analyzed by the microplate reader and detected at the absorbance of 490 nm. The cell viability (%) = $(OD_{sample} - OD_{blank}) / (OD_{control} - OD_{blank}) \times 100$ %. (OD_{sample}, $OD_{control}$, and OD_{blank} denote the cells incubated with various concentrations of the **QV-S**, the cells without the **QV-S**, and the wells containing only the culture media, respectively). RAW264.7 cells showed more than 90% cell viability below the **QV-S** concentration of 10 μM, which suggested **QV-S** has low cytotoxicity to live cells at a specific concentration. Therefore, we selected 10 μM as the maximum dosage for the subsequent cellular experiments.

Cell Imaging

Co-localization Experiment

The lysosomes-targeting performance of probe **QV-S** was tested with the

colocalization experiments by costaining the RAW264.7 cells with Lysotracker Green (a typical commercially available lysosomes tracker) and probes. The RAW264.7 cells were incubated with Lysotracker Green (3 μM) for 2h and then with **QV-S** probes (10 μM) for 30 min, λ_{ex} = 488 nm, harvesting wavelength of 508-580 nm. Lipid droplet were localized using Nile Red (3 μM incubated for 30 min), λ_{ex} = 561 nm, harvesting wavelength of 585-650 nm. Mitochondrial were localized using MitoTracker Green (150 nM incubated for 30 min), λ_{ex} = 633 nm, harvesting wavelength of 700-850 nm. Nucleus were localized using Hoechst 33342 (10 μM incubated for 30 min), λ_{ex} = 405 nm, harvesting wavelength of 415-450 nm, cells were rapidly imaged under a sp8 confocal microscope.

Cell Imaging Assays of Lysosomal Viscosity Changes under Dexamethasone Stimulation

To conduct fluorescence imaging of lysosomal viscosity changes in RAW264.7 cells, Dexamethasone (DXMS, 5 μM) were added to the inoculum with RAW264.7 cells and incubated for 15 min before adding 10 μM **QV-S**. Confocal fluorescence imaging of RAW264.7 cells was measured through the bright field and red fluorescence channel.

Cell Imaging Assays of Cell Viscosity Changes under Drug Stimulation

To conduct fluorescence imaging of cell viscosity changes in RAW264.7 cells, nystatin (10 μM) or lipopolysaccharides (10 μg / mL) were added to the inoculum with RAW264.7 cells and incubated for 30 min before adding 10 μM probe **QV-S**. H_2O_2 (50 μM) was added to the inoculum with RAW264.7 cells and incubated for 30 min or 60 min before adding 10 μM probe **QV-S**. Confocal fluorescence imaging of RAW264.7 cells was measured through the bright field and red fluorescence channel.

Cell Imaging Assays of Cell Viscosity Changes induced by Oxidized Low-density Lipoprotein with QV-S

Oxidized low density lipoprotein (ox-LDL) can induce RAW264.7 cell macrophages to produce foam cells. After cell adhesion, ox-LDL (10 μM) was used to induce cells at 0 h, 6 h, 12 h, 24 h, and 48 h before adding the probe **QV-S** (10 μM) or commercial probe Nile red (3 μM).

In Vitro Imaging of Atherosclerosis Mouse Aorta

A high-fat diet was used to feed ApoE deficient (*ApoE*$^{-/-}$) mice for 8 weeks to establish an early AS mouse model as the experimental group, and C57BL/6 mice of the same gender and age were used as the control group. Three control group and experimental group mice were respectively selected, and the **QV-S** (50 μ M, 75 μL) was intravenously injected. After 3 hours, blood was collected from the eyeballs, and serum samples were taken to measure the four levels of blood lipids (triglycerides, cholesterol, high-density lipoprotein cholesterol, low-density lipoprotein cholesterol); Dissect the aorta of mice, remove excess fat, and place it in a live imaging device for imaging; After imaging is completed, the blood vessels are segmented and embedded in a mold for frozen sectioning. After sectioning, confocal imaging is performed.

2. Synthesis of QV-S

Synthesis of compound **1**. The 4-Bromo-2-hydroxybenzaldehyde (2.41g, 11.9mmol), cesium carbonate (5g,15.3mmol) and 2-bromocyclohex-1-ene-1-carbaldehyde (3g，15.8 mmol) were dissolved in anhydrous N, N-dimethylformamide (15 mL). This mixture was stirred at room temperature for 16 h. After the TLC monitoring reaction was completed, filter and add saturated sodium chloride solution, the aqueous layer was extracted with a further 2 portions of dichloromethane (25 mL). The combined organic fractions were dried over anhydrous Na_2SO_4. and the solvent was removed in vacuo to yield the deprotected amine as a yellow oil. Removal of solvent and recrystallization from EtOAc and hexane gave compound **1** (2.5 g, 54%). ^{1}H NMR (400 MHz, $CDCl_3$) δ 10.31 (d, *J* = 2.6 Hz, 1H), 7.30-7.27 (m, 1H), 7.20 (dd, *J* = 8.1, 1.8 Hz, 1H), 7.02 (dd, *J* = 8.1, 1.7 Hz, 1H), 6.62 (s, 1H), 2.62-2.54 (m, 2H), 2.44 (dd, *J* = 8.3, 3.7 Hz, 2H), 1.76-1.69 (m, 2H). ^{13}C NMR (101 MHz, $CDCl_3$) δ 187.90, 159.51, 152.31, 130.28, 127.54, 126.96, 125.64, 122.94, 120.24, 118.76, 113.82, 30.14, 21.44, 20.18. HRMS: (ESI, m/z) Calcd for $C_{14}H_{11}BrO_2$ $[M+H]^+$: 291.0007, found 291.0015.

Synthesis of compound **3**. The compound **1** (600 mg, 2.06 mmol), compound **2** (4-Methyldiphenylamine, 480 mg, 2.41 mmol), cesium carbonate (1.662 g, 5.1 mmol),

Pd_2 $(dba)_3$ (84 mg, 0.09 mmol), and DavePhos (65 mg, 0.17 mmol) were dissolved in dioxane solution (13 ml). This mixture was stirred at 95℃ for 18 h under argon protection. After the TLC monitoring reaction was completed, filter and vacuum concentrate the filtrate. Then add ethyl acetate to precipitate an orange red solid (0.55 g, 65%). ^{1}H NMR (400 MHz, $CDCl_3$) δ 10.17 (s, 1H), 7.29 (t, *J* = 7.9 Hz, 2H), 7.13-7.07 (m, 5H), 6.96 (d, *J* = 8.9 Hz, 1H), 6.88 (d, *J* = 8.9 Hz, 2H), 6.67 (d, *J* = 7.4 Hz, 2H), 6.63 (s, 1H), 3.82 (s, 3H), 2.59-2.53 (m, 2H), 2.43 (t, *J* = 6.0 Hz, 2H), 1.73-1.67 (m, 2H). ^{13}C NMR (101 MHz, $CDCl_3$) δ 187.30, 161.09, 157.07, 153.21, 150.27, 146.78, 139.43, 129.48, 128.01, 127.10, 126.18, 124.79, 123.84, 116.17, 115.06, 114.70, 112.27, 106.46, 55.51, 29.99, 21.56, 20.53. HRMS: (ESI, m/z) Calcd for $C_{27}H_{23}NO_3$ $[M+H]^+$: 410.1733, found 410.1750.

Synthesis of compound **4**. The 4-methylquinoline (1.52 g, 10.6 mmol) and 1,3-propanesultone (1.25 g, 10.2 mmol) were dissolved in toluene solvent (5 mL). This mixture was stirred at 110℃ for 1.5 h under argon protection. The solution changed from colorless to a white oily liquid, and after cooling, it was washed with ether to obtain a white solid (2.4 g, 86%). ^{1}H NMR (400 MHz, D_2O) δ 9.07 (d, *J* = 6.1 Hz, 1H), 8.41 (dd, *J* = 17.7, 8.7 Hz, 2H), 8.19 (t, *J* = 8.0 Hz, 1H), 7.96 (t, *J* = 7.7 Hz, 1H), 7.88 (d, *J* = 6.0 Hz, 1H), 5.17-5.07 (m, 2H), 3.07 (t, *J* = 7.1 Hz, 2H), 2.99 (s, 3H), 2.55-2.44 (m, 2H). ^{13}C NMR (101 MHz, D_2O) δ 160.01, 147.36, 137.12, 135.43, 129.58, 126.98, 122.48, 118.33, 55.73, 47.37, 24.73, 19.52. HRMS: (ESI, m/z) Calcd for $C_{13}H_{15}HO_3S$ $[M+H]^+$: 266.0849, found 266.0845.

Synthesis of **QV-S**. The compounds **3** (205 mg, 0.5 mmol) and **4** (398 mg, 1.5 mmol) were dissolved in acetic anhydride (12 mL). This mixture was stirred at 110℃ for 1 h under argon protection. After the completion of TLC monitoring reaction, add water, the aqueous layer was extracted with a further 2 portions of dichloromethane (25 mL). The solvent was removed in vacuo, and the residue was purified by silica gel chromatography (DCM: MeOH = 10 : 1) to afford **QV-S** as blue green solid (0.28 g, 84%). ^{1}H NMR (400 MHz, DMSO-d_6) δ 8.95 (d, *J* = 6.8 Hz, 1H), 8.80 (d, *J* = 8.5 Hz, 1H), 8.47 (d, J = 8.9 Hz, 1H), 8.40 (d, J = 15.1 Hz, 1H), 8.29 (d, J = 6.9 Hz, 1H),

8.16-8.08 (m, 1H), 7.93-7.80 (m, 1H), 7.34 (dd, J = 20.1, 12.2 Hz, 3H), 7.18 (d, J = 8.4 Hz, 1H), 7.10 (dd, J = 11.6, 5.7 Hz, 5H), 6.99 (d, J = 9.0 Hz, 2H), 6.92 (d, J = 2.0 Hz, 1H), 6.88 (s, 1H), 6.57 (dd, J = 8.3, 2.2 Hz, 1H), 4.96 (t, J = 7.2 Hz, 2H), 3.78 (s, 3H), 2.71 (s, 2H), 2.60 (s, 2H), 2.28-2.13 (m, 2H), 1.80 (s, 2H), 1.24 (s, 2H). HRMS: (ESI, m/z) Calcd for $C_{40}H_{36}N_2O_5S$ $[M+H]^+$: 657.2405, found 657.2417.

3. Supplemental scheme and figures

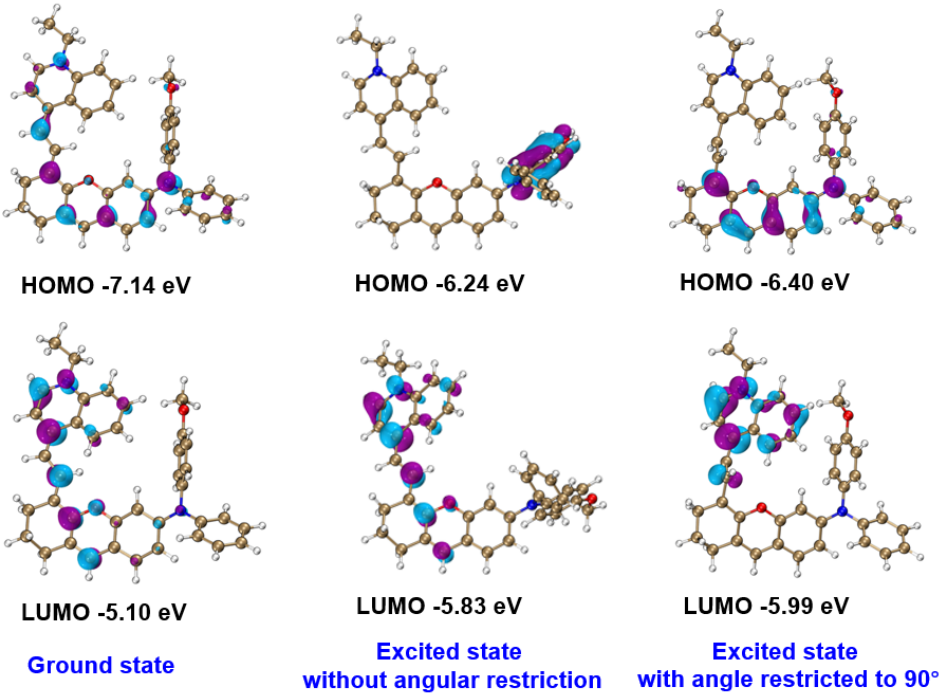

Fig. S1 HOMO and LUMO of ethylated **QS-V** at the minimum energy structures of compound 3 in electronic ground and excited states. Geometries were optimized at the B3LYP-D3/6-31G(d) level.

Since molecules containing sulfonic acid groups are difficult to converge during the optimization of excited states and do not directly affect luminescence properties, they were simplified to ethyl groups. DFT calculations indicate that photoexcitation of ethylated **QS-V** from the S_0 to the S_1 state is primarily governed by electron transitions from the highest occupied molecular orbital (HOMO) to the lowest unoccupied molecular orbital (LUMO). The HOMO is largely localized on the triphenylamine group, whereas the LUMO is mainly situated on the quinolinium unit.

The frontier molecular orbital diagram reveals a distinct charge transfer from the triphenylamine moiety to the quinolinium unit, indicative of a typical twisted intramolecular charge transfer (TICT) process. Based on the discussion above, it can be concluded that **QS-V** functions as an excellent viscosity-sensitive fluorescent probe operating via the TICT mechanism.

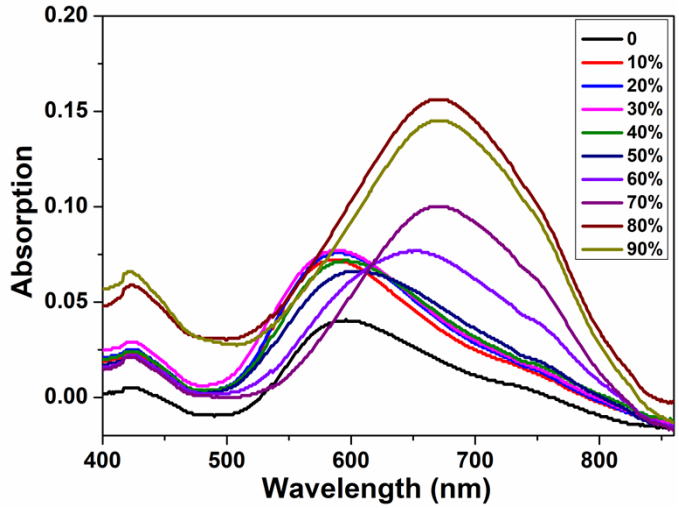

Fig. S2 Absorption spectra of **QV-S** (10 μM) in glycerol/PBS mixtures of various fractions (0-90%).

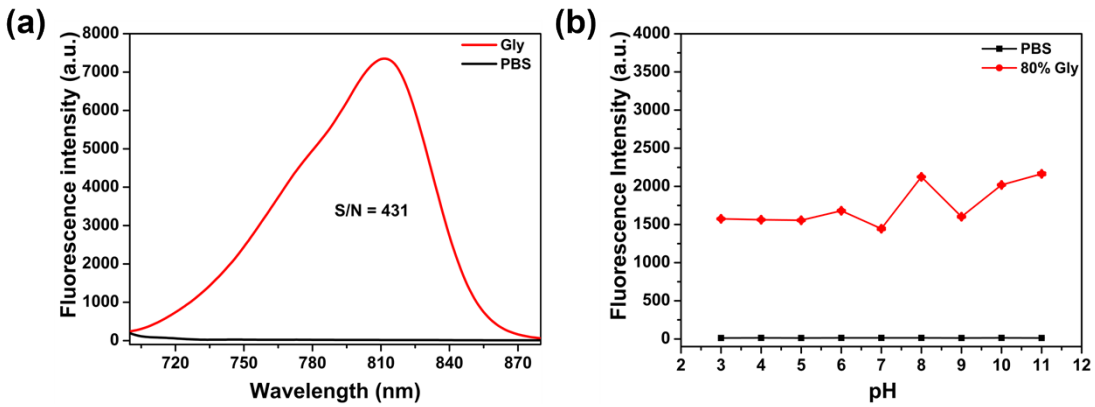

Fig. S3. (a) Fluorescence spectra of **QV-S** (10 μM) in various volume ratios of PBS and glycerol mixture (0 % and 99 %). (b) Fluorescence intensity of probe **QV-S** (10 μ M) under different pH = 3-11 conditions in 80% Gly and PBS.

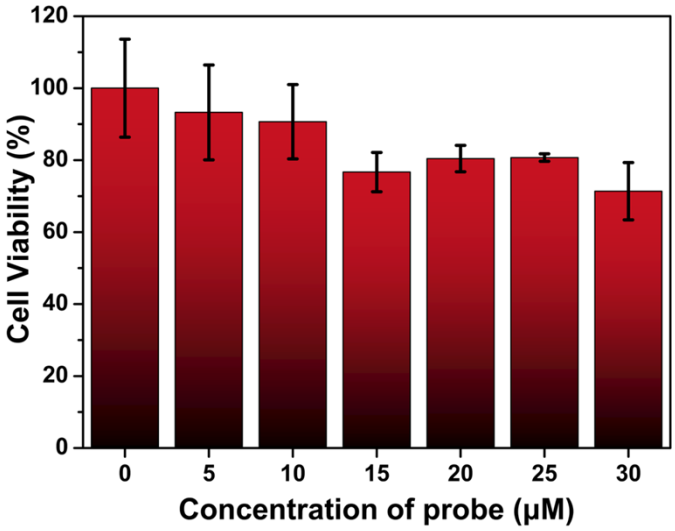

Fig. S4. MTT assay of RAW264.7 cells in the presence of different concentrations of **QV-S**

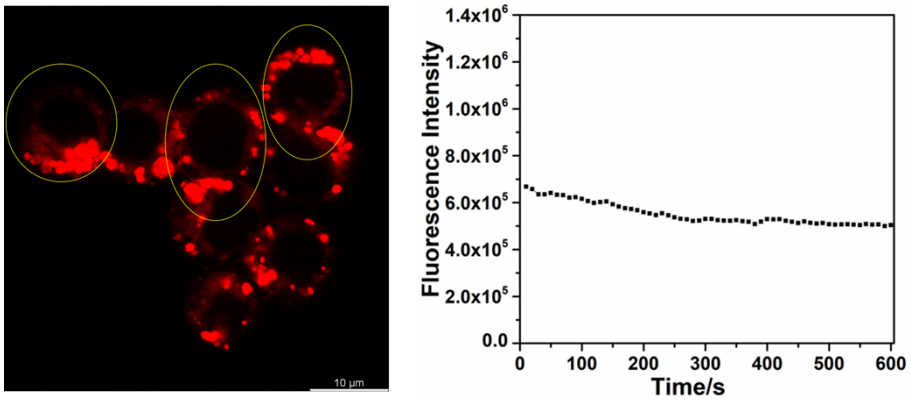

Fig. S5. Test of photostability of **QV-S** in RAW264.7 cells. Confocal fluorescence images (0-600 s) were achieved by means of time-sequential scanning of the **QV-S** (10 μ M)-loaded RAW264.7 cells. (λ_{ex} = 633 nm, collected 700-850 nm, Scale bar = 10 μm)

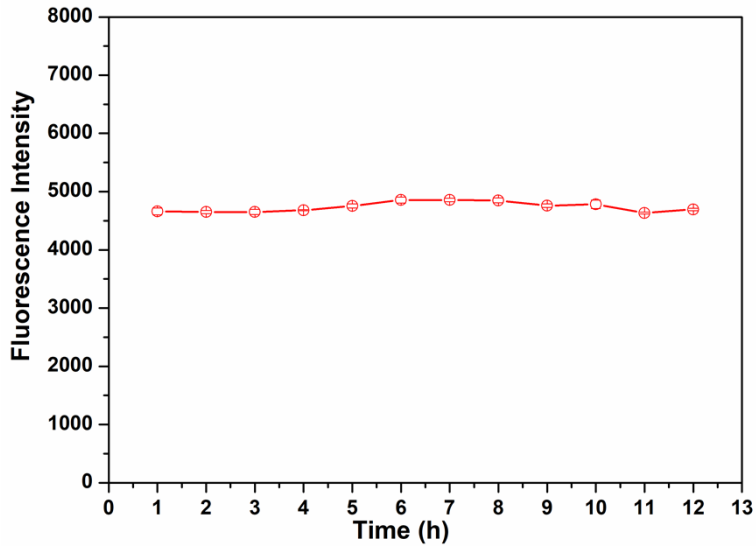

Fig. S6. Test of stability of **QV-S** in serum. Fluorescence of **QV-S** (10 μM) in serum at different time points (1-12 hours).

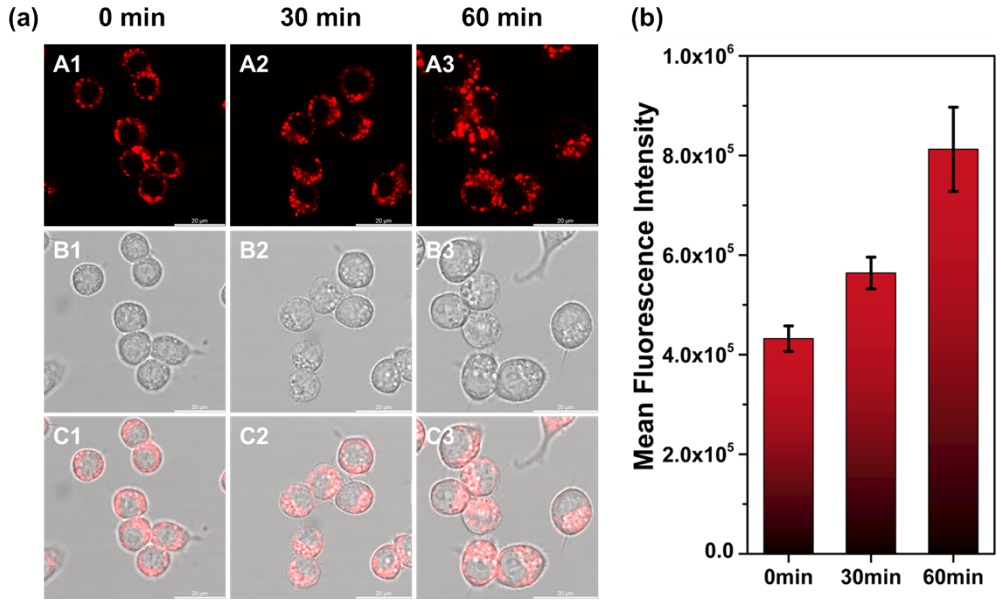

Fig. S7. (a) Fluorescence images of **QV-S** in RAW264.7 cells induced by H_2O_2 (50 μM). (b) Relative fluorescence intensities of the images in panel a. (λ_{ex} = 633 nm, collected 700-850 nm, Scale bar = 20 μm.)

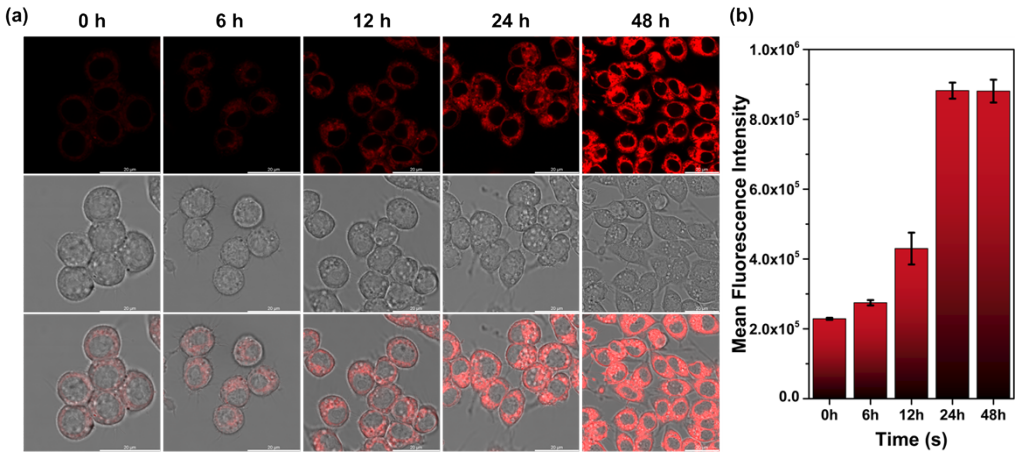

Fig. S8. (a) Confocal imaging of commercial probe **Nile Red** (3 μ M) induced by ox-LDL (10 μM) in RAW264.7 cells (b) Relative fluorescence intensities of the images in panel a. (λ_{ex} = 561 nm, collected 585-650 nm, Scale bar = 20 μm.)

Table S1 Four values of blood lipida in mice (mmol / L)

Sample Name	triglyceride	cholesterol	High-density lipoprotein cholesterol	Low density lipoprotein cholesterol
C57BL/6	0.921	2.281	1.378	0.312
ApoE$^{-/-}$	1.571	22.630	2.350	12.146

Table S2 Detection parameters of small molecule fluorescent probes for viscosity

Probe Name	Excitation Wavelength (nm)	Stokes shift (nm)	Fluorescence enhancement	Targeting organelle	Biological application	Ref
NIR-V	700	120	22-fold	Mitochondria	Diabetic mice	22
DCO-5	620	185	180-fold	No	Zebrafish	23
CS-PyBC	650	180	92-fold	Mitochondria	HeLa cells Mitophagy	24
GA-Vis	515	27	12-fold	Golgi	Alcohol-induced liver injury	25
MYN-BS	710	40	36-fold	Cell membrane	Cell foaming	26
Probe unnamed	599	64	55-fold	Cell membrane	HeLa cells	27
Cy-914	795	225	72-fold	Mitochondria	Non-alcoholic fatty liver	28
IC-V	700	170	180-fold	No	Tumor-bearing mice	29
Probe unnamed	534	44	25-fold	Lysosomes	SH-SY5Y cells	30
$N(CH_2)_3$-BD-PZ	541	163	20.5-fold	Lysosomes	HeLa cells	31
Lyso-vis-A	590	120	160-fold	Lysosomes	HEK293 and HeLa cells	32
N(CH2)3-PD-NEt	615	200	90-fold	Mitochondria	Apoptosis process of HepG2 cells	33
Probes 6	594	83	5-fold	Lysosomes	HeLa cells	34
QV-S	**815**	**135**	**431-fold**	**Lysosomes**	**Atherosclerotic plaques**	**Our work**

4. References

[1] M.J. Frisch, et al., Gaussian 16, Revision C.01, Gaussian, Inc., Wallingford, CT, 2016.

[2] S. Grimme, et al., A consistent and accurate ab initio parametrization of density functional dispersion correction (DFT-D) for the 94 elements H-Pu, *J. Chem. Phys.*, 2010, 132, 154104.

[3] T. Lu, F. Chen, Multiwfn: A multifunctional wavefunction analyzer, *J. Comput. Chem.*, 2012, **33**, 580-592.

[4] W. Humphrey, et al., VMD: Visual molecular dynamics, *J. Mol. Graph.*, 1996, **14**, 33-38.

5. ^{1}H NMR, ^{13}C NMR and HR MS spectra

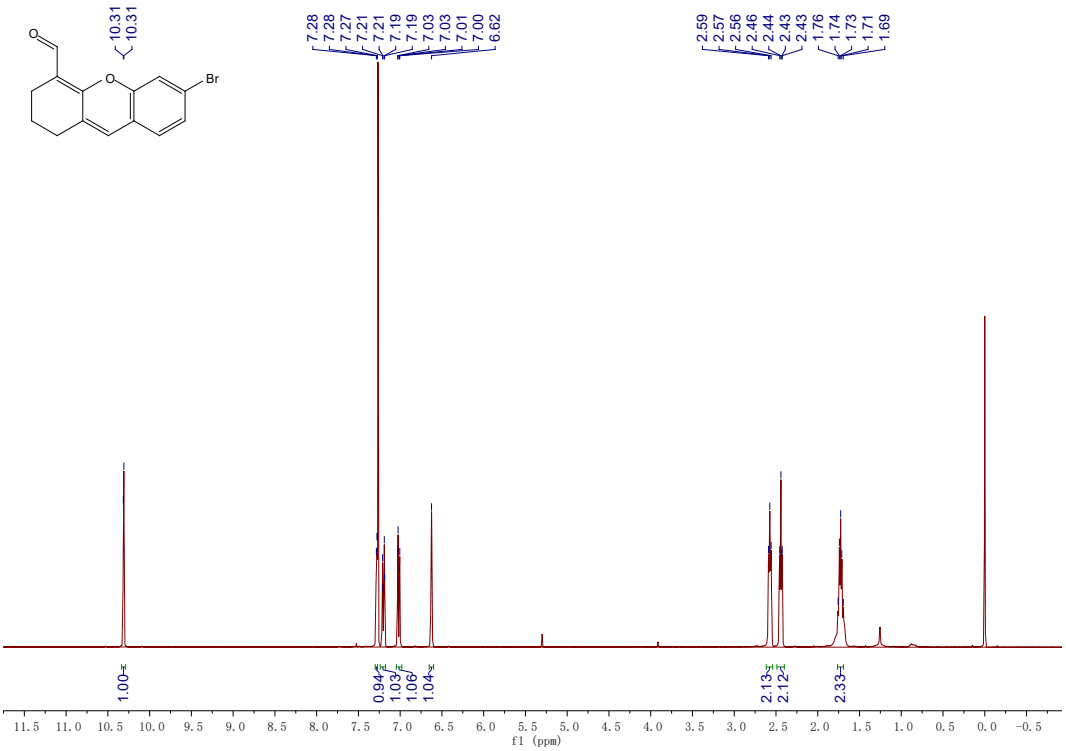

Fig. S9 ^{1}H-NMR spectrum of compound **1** in $CDCl_3$ (400 MHz).

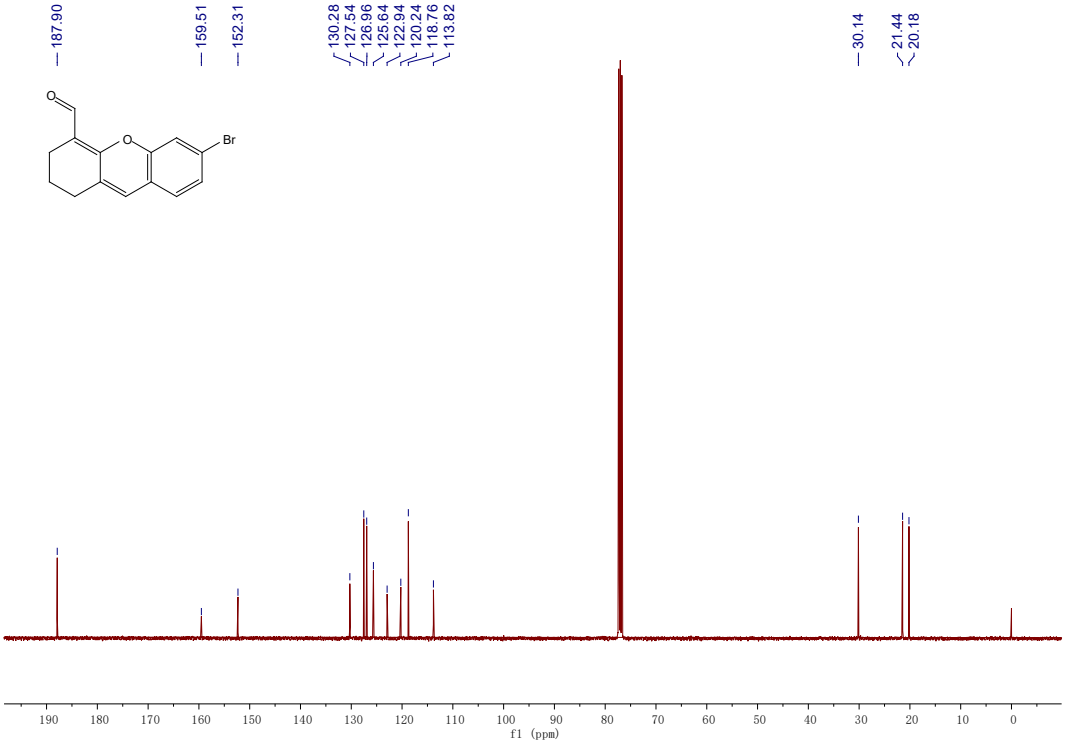

Fig. S10 ^{13}C-NMR spectrum of compound **1** in $CDCl_3$ (101 MHz).

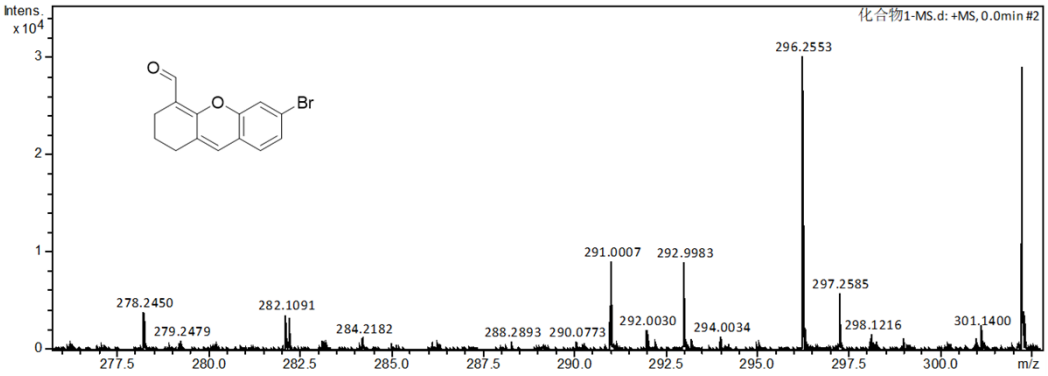

Fig. S11 HR MS spectrum of compound **1**.

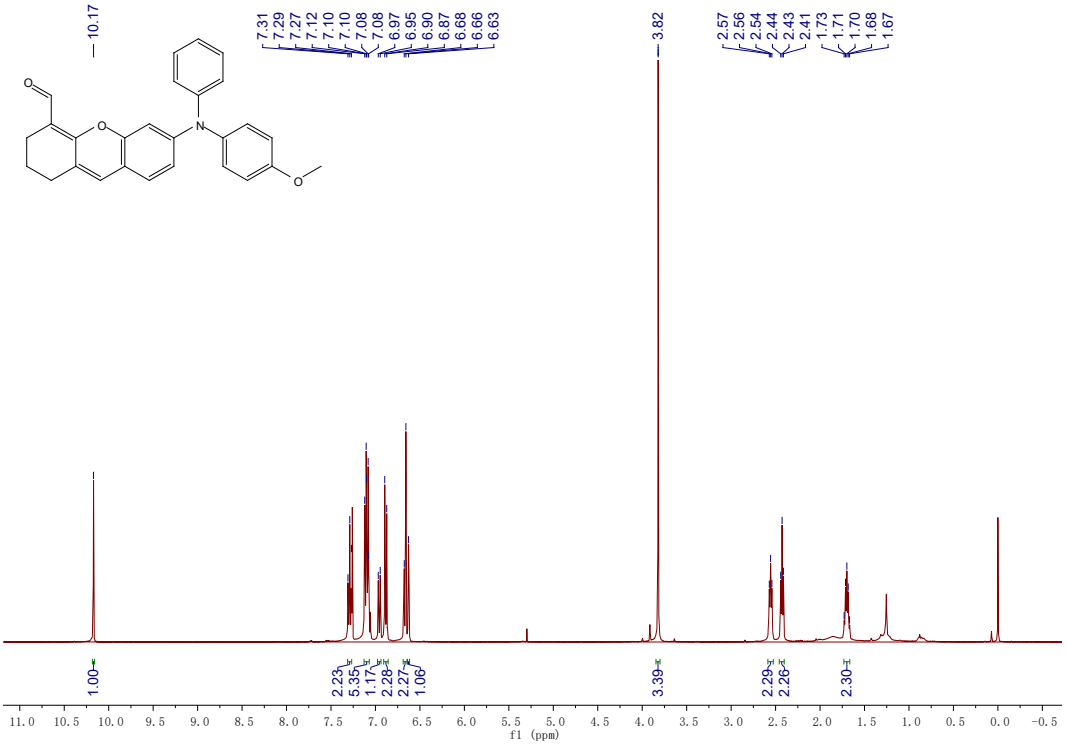

Fig. S12 ^{1}H-NMR spectrum of compound **3** in $CDCl_3$ (400 MHz).

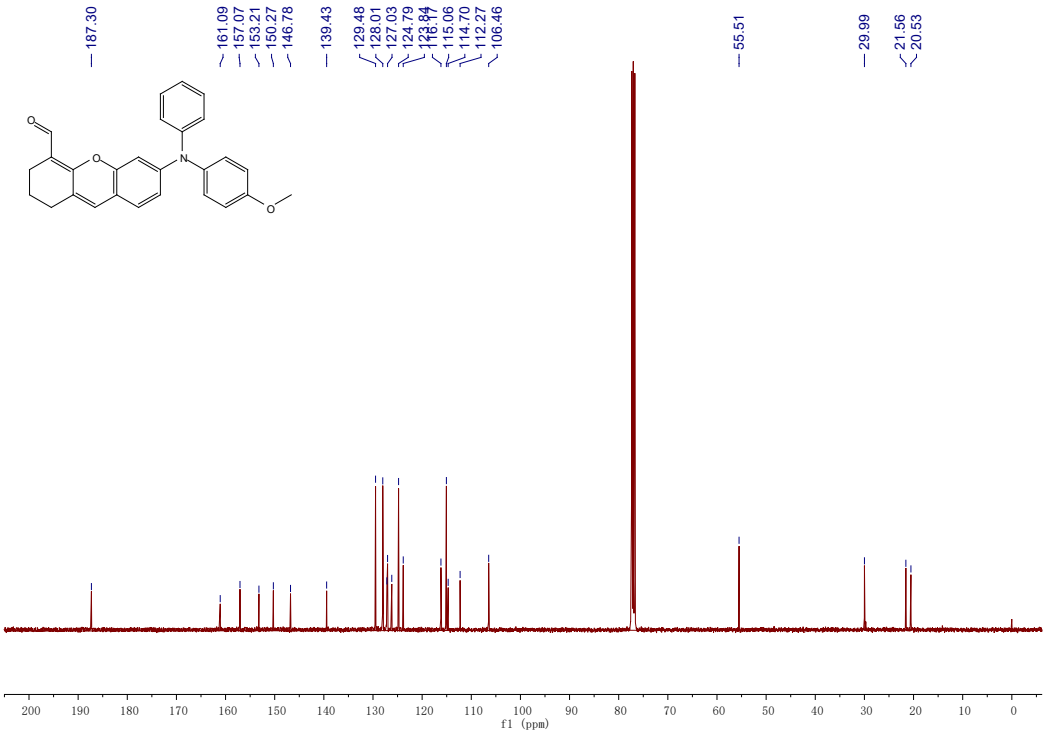

Fig. S13 ^{13}C-NMR spectrum of compound **3** in $CDCl_3$ (101 MHz).

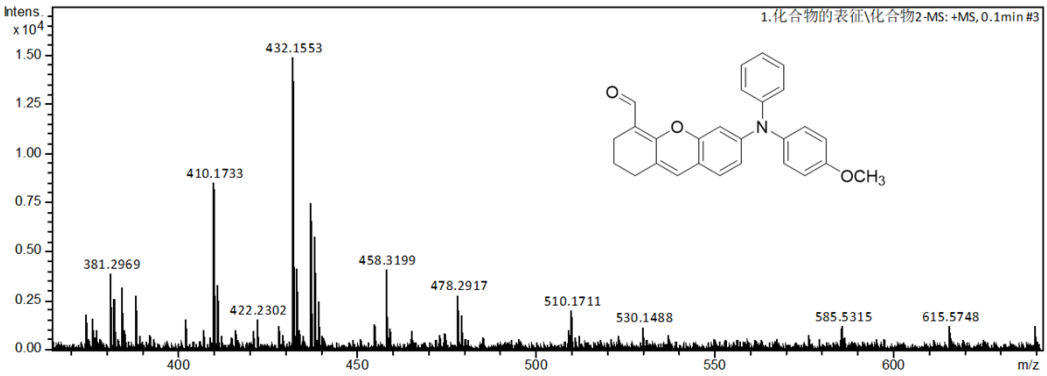

Fig. S14 HR MS spectrum of compound **3**.

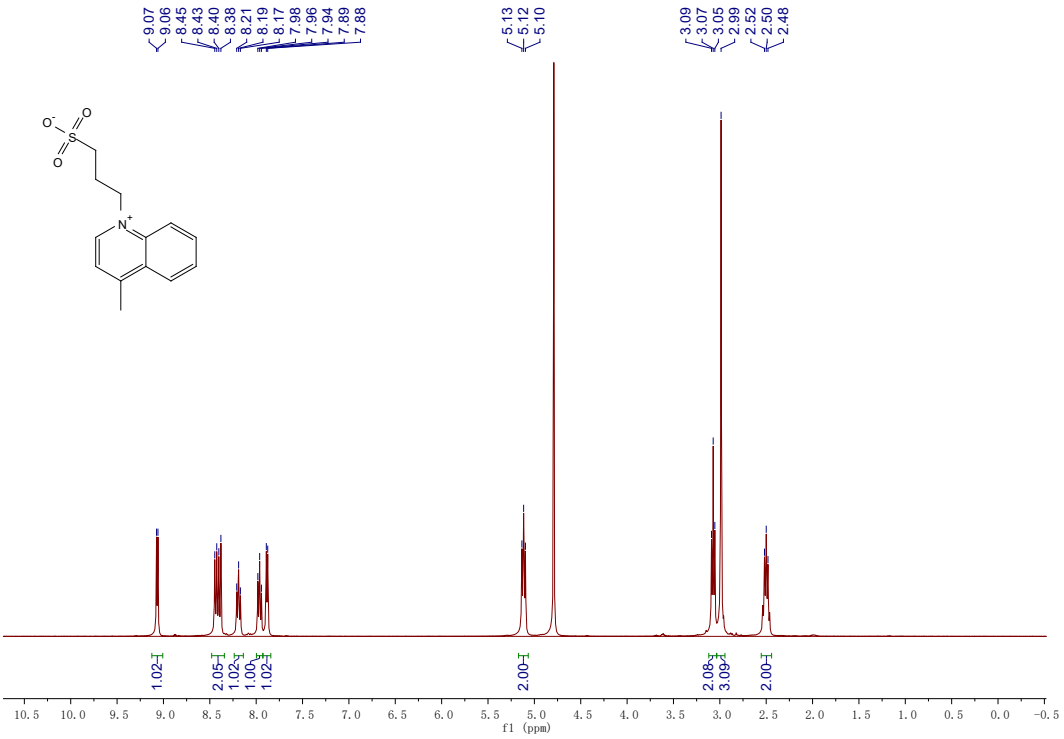

Fig. S15 ^{1}H-NMR spectrum of compound **4** in D_2O (400 MHz).

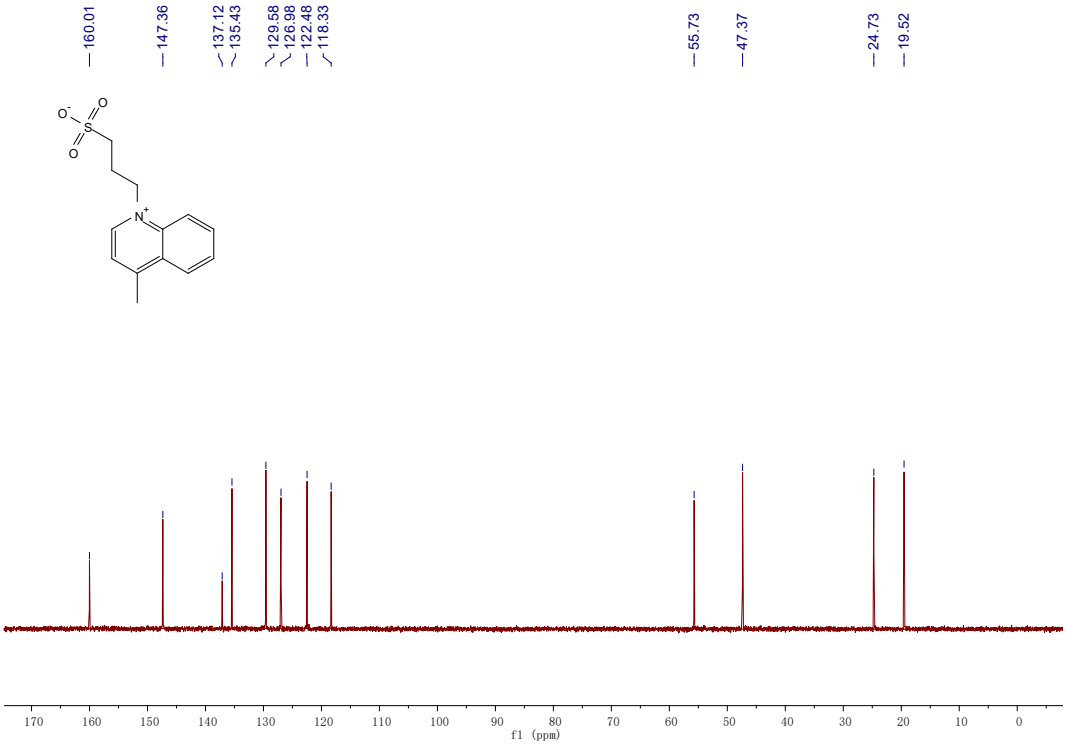

Fig. S16 ^{13}C-NMR spectrum of compound **4** in D_2O (101 MHz).

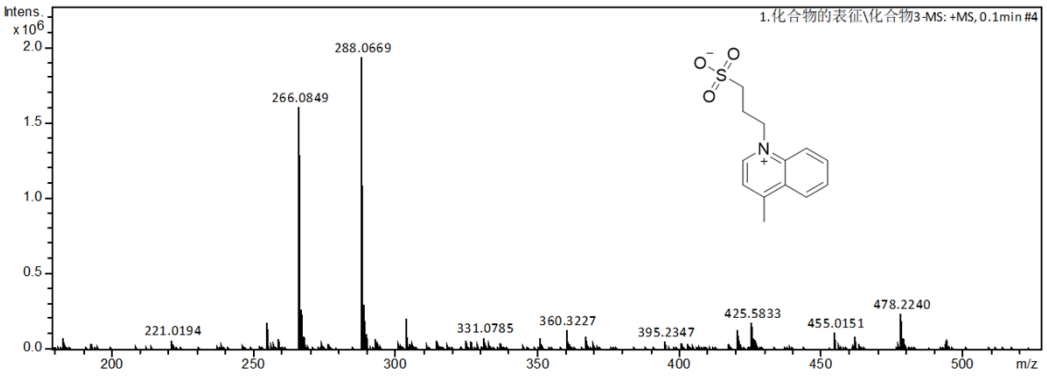

Fig. S17 HR MS spectrum of compound **4**.

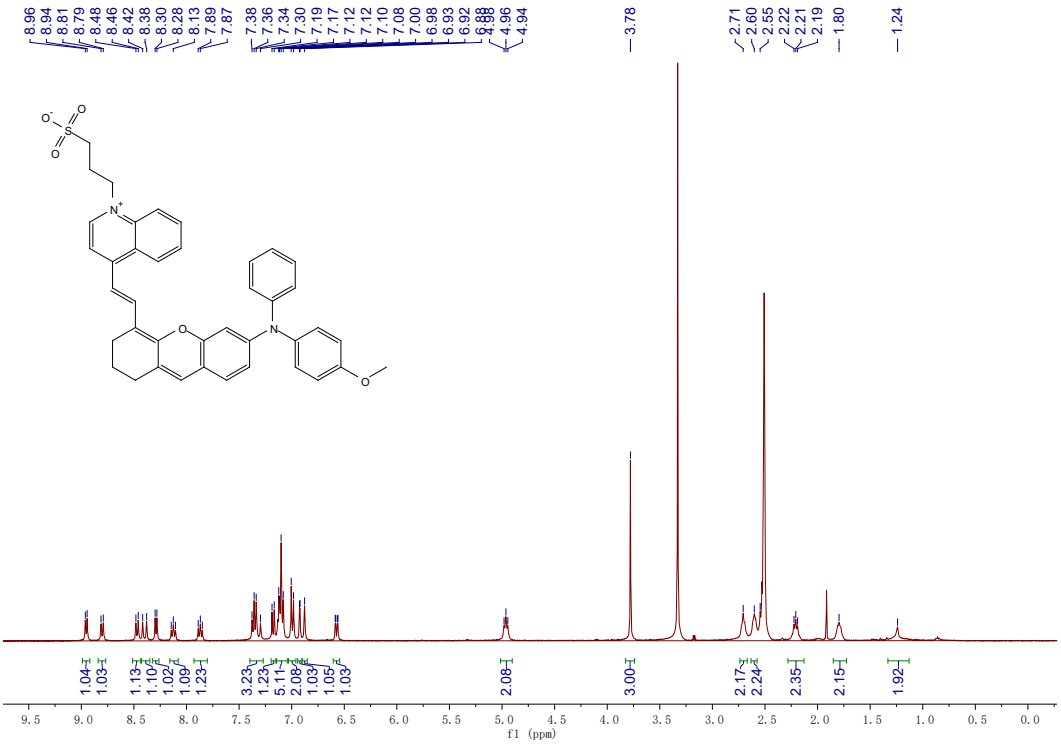

Fig. S18 ^{1}H-NMR spectrum of **QV-S** in DMSO-d_6 (400 MHz).

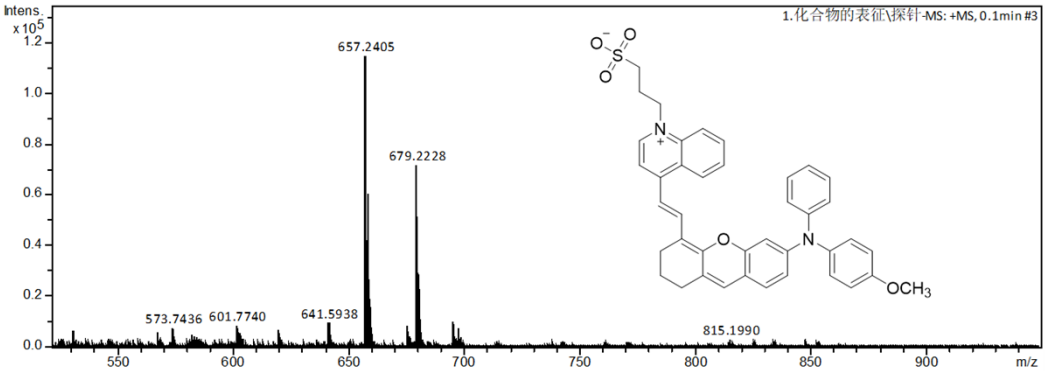

Fig. S19 HR MS spectrum of **QV-S**.